Obenschain

The Pennsylvania State University
APPLIED RESEARCH LABORATORY
P.O. Box 30
State College, PA 16804

Shearography for
Non-destructive Inspection
with applications to
BAT Mask Tile Adhesive Bonding and
Specular Surface Honeycomb Panels

by: Daniel B. Lysak

Technical Report No. TR 03 - 005
March 2003

Abstract

The applicability of shearography techniques for non-destructive evaluation in two unique application areas is examined. In the first application, shearography is used to evaluate the quality of adhesive bonds holding lead tiles to the BAT gamma ray mask for the NASA Swift program. Using a vibration excitation, the more poorly bonded tiles are readily identifiable in the shearography image. A quantitative analysis is presented that compares the shearography results with a destructive pull test measuring the force at bond failure.

The second application is to evaluate the bonding between the skin and core of a honeycomb structure with a specular (mirror-like) surface. In standard shearography techniques, the object under test must have a diffuse surface to generate the speckle patterns in laser light, which are then sheared. A novel configuration using the specular surface as a mirror to image speckles from a diffuser is presented, opening up the use of shearography to a new class of objects that could not have been examined with the traditional approach. This new technique readily identifies large scale bond failures in the panel, demonstrating the validity of this approach.

TABLE OF CONTENTS

LIST OF FIGURES

Executive Summary

In this report we examine the applicability of shearography techniques for non-destructive inspection and evaluation in two unique application areas. In the first application, shearography is used to evaluate the quality of adhesive bonds holding lead tiles to the BAT gamma ray mask for the NASA Swift program. By exciting the mask with a vibration, the more poorly bonded tiles can be distinguished by their greater displacement response, which is readily identifiable in the shearography image. A quantitative analysis is presented that compares the shearography results with a destructive pull test measuring the force at bond failure. Generally speaking, the results show good agreement. Further investigation would be useful to optimize certain test parameters such as vibration frequency and amplitude.

The second application is to evaluate the bonding between the skin and core of a honeycomb structure with a specular (mirror-like) surface. In standard shearography techniques, the object under test must have a diffuse surface to generate the speckle patterns in laser light, which are then sheared. A novel configuration using the specular surface as a mirror to image speckles from a diffuser is presented, opening up the use of shearography to a new class of objects that could not have been examined with the traditional approach. This new technique readily identifies large scale bond failures in the panel, demonstrating the validity of this approach.

For the particular panel examined here, some scaling issues should be examined further to resolve the measurement scale down to the very small size of the core cells. In addition, further development should be undertaken to determine the general applicability of the new approach and to establish a firm quantitative foundation.

1. Introduction

The goal of this project is to evaluate the applicability of shearography for nondestructive inspection and evaluation (NDI / NDE) of certain mission critical components. This work was performed as part of a Cooperative Agreement with the NASA Goddard Space Flight Center (GSFC), grant number NCC5-508. Two potential application areas were identified:

> 1. For tiles on the Swift BAT gamma ray mask, to determine whether poorly-bonded tiles could be distinguished from well-bonded tiles.
> 2. To determine whether shearography could identify any bonding failure between the skin and the core of specular-surface honeycomb structures.

The Penn State University Applied Research Lab (PSU/ARL) provided the shearography system and labor while the GSFC provided the test samples and consultation regarding sample construction and appropriate test environments.

Shearography, a form of speckle shear interferometry, is a robust yet sensitive technique for NDI / NDE that has been demonstrated to be effective in the field environment out of the laboratory. [1] Unlike holographic methods, which measure absolute surface displacements and are very sensitive to environmental disturbances, shearography is a differential technique that measures changes in surface gradient due to applied excitation stress. As such, it provides a common mode rejection that makes it relatively insensitive to environmental conditions. While shearography has been around for some time, the phase shifting technique used in the PSU/ARL system provides greatly improved visualization of results by computing the speckle phase instead of merely using the speckle image, as in earlier methods. [2]

The two application areas require different methods of generating the excitation stress. In the case of the BAT mask tiles, the adhesive holding the tile is somewhat flexible, and if we apply a low amplitude vibration in the plane of the mask, the tile tends to tilt back and forth slightly. The amplitude of this motion depends inversely on how well the tile is bonded to the surface of the mask. By taking two snapshots, 180° apart at the extremes of the tile vibration cycle, the shearography system measures the amplitude of motion as the change in slope of the tile surface.

For honeycomb panels shearography has been demonstrated to give good results in identifying bonding failures between the core and skin under vacuum, pressure, and even thermal excitation. At the cell walls of the honeycomb core, where the skin is attached, the surface is constrained, and there is no change in the surface slope when the excitation is applied. However, at the interior of the cells there is nothing holding the skin, so the surface slope is free to change under the excitation, and, when the differential surface gradient is displayed, it will appear different from the constrained areas. If the structure is sound, the distinct honeycomb pattern of the core will appear in the display, and any bonding failure will be readily apparent as an interruption of that pattern. In the present application, however, the challenge is that the panels have a specular (mirror-like) finish and do not produce the speckle patterns needed for shearography. (Note that the terms "specular" and "speckle" have an unfortunate phonetic similarity which can often be the

source of some confusion.) In this case the speckles can be generated by illuminating some other diffuse surface with laser light and then use the specular surface as a mirror to view them. In principle, this configuration should produce a display very similar to that obtained from a diffuse surface honeycomb panel.

In Section 2 below, we review the principles of shearography and describe the basic PSU/ARL system configuration and operation. In Sections 3 and 4 we discuss in detail the two application areas, the BAT mask tiles and the specular honeycomb panel, respectively. These sections include the experimental set up for each case and results obtained. Finally in Section 5 we present our conclusions and recommendations.

2. Technical Background

Shearography makes use of the "subjective" speckle pattern [3] that is produced through random interference when the rough surface of an object is illuminated by coherent laser light and imaged through a lens. The speckle image is "sheared" by splitting the wave front into two parts which are then recombined at the image plane with a small transverse shift between them. The effect is that each point in the image plane is the image of two different scattering points on the rough surface separated by the shear vector (δx, δy). The speckle intensity at the image point depends on the interference between these two scattering points. The speckle pattern produced is highly sensitive to differential out-of-plane displacements over the shear distance but relatively insensitive to common mode displacements. As a result, shearography provides a technique for measuring small changes in surface slope that is robust enough to operate outside the laboratory environment.

The PSU/ARL shearography system is illustrated in Figure 1 below. It uses a Coherent DPSS-532 diode-pumped Nd:YAG continuous wave (CW) laser producing 500 mW output at 532 nm as the illumination source with a Pulnix TM-1040 Progressive Scanning High Resolution camera (960 x 640 pixels) interfaced through a Bitflow RoadRunner frame grabber to record the speckle images. Speckle shearing is produced using a Michelson interferometer arrangement with one of the mirrors tilted, and the shear distance is set by adjusting the degree of tilt. A 486-based lunchbox computer is used to acquire the camera images, process the data, and display the results as well as for overall control and synchronization of the various subsystems.

Generally speaking, nondestructive evaluation is done by observing the changes when some small excitation is applied to the object under test. Various types of excitation, such as pressure, heat, force, vibration, and others, may be used depending on the particular application. With shearography, the changes in the observed speckle pattern infer changes in the surface gradient component in the direction of the shear displacement. Two speckle images, representing the reference and excited states, can be subtracted to produce a visualization of the gradient changes. However, better immunity to variations in surface reflectivity and other noise effects can be obtained by first obtaining the speckle phase at each pixel for both the reference and the excitation

conditions, and then computing the phase difference pixel by pixel. This produces a much clearer visualization image, and the result is a more quantitative representation of the change in gradient.
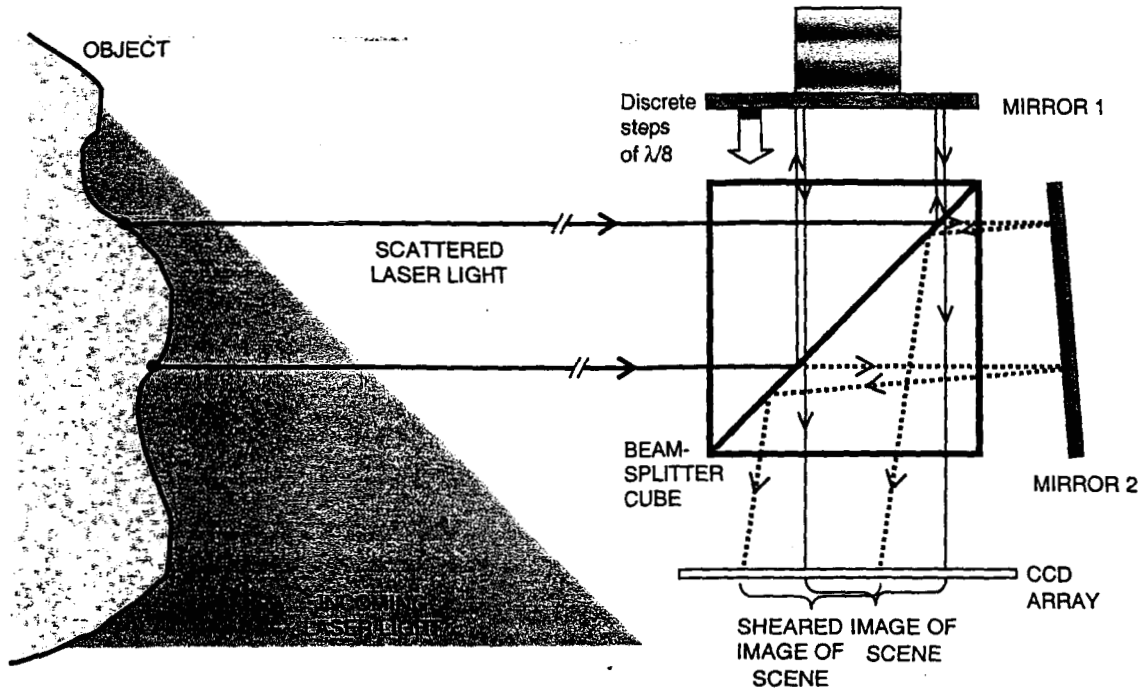
Figure 1. Basic PSU/ARL shearography configuration, based on a Michelson interferometer with phase stepping. The piezo-electric actuator (PZT) controls the stepping of mirror 1, while the shear distance is determined by the tilt in mirror 2. The imaging lens, located between the beam splitter cube and the CCD array, is not shown.

In the PSU/ARL shearography system, speckle phase is computed using a highly accurate, four-step, phase-stepping approach in which four separate images are taken at different interferometric path differences, in quarter wavelength increments. Phase stepping is performed by moving one of the interferometer mirrors (mirror 1 in Figure 1) using a piezo-electric actuator controlled by a waveform generator board in the computer. The intensity at pixel (x,y) in each of the four images can be represented by

$$I_1(x, y) = a(x, y) + b(x, y)\cos[\phi(x, y)]$$

$$I_2(x, y) = a(x, y) + b(x, y)\cos[\phi(x, y) + \pi/2]$$

$$I_3(x, y) = a(x, y) + b(x, y)\cos[\phi(x, y) + \pi]$$

$$I_4(x, y) = a(x, y) + b(x, y)\cos[\phi(x, y) + 3\pi/2], \quad (1)$$

where $\varphi(x,y)$ is the speckle phase, which is directly related to differential optical path length through the two scattering points. The bias intensity, $a(x,y)$, and fringe modulation intensity, $b(x,y)$, account for variations in illumination, surface reflectivity, and other effects. Solving for the speckle phase, the $a(x,y)$ and $b(x,y)$ terms drop out of the solution, and we get

4

$$\varphi(x,y) = \tan^{-1}\left[\frac{I_2(x,y) - I_4(x,y)}{I_1(x,y) - I_3(x,y)}\right]. \tag{2}$$

If the shearing distance is small and the illumination and viewing directions are nearly normal to the object surface, the change in speckle phase can be approximately related to the differential displacement by

$$\Delta\phi(x,y) = \phi_e(x,y) - \phi_r(x,y)$$
$$= \frac{4\pi}{\lambda}(\delta z_e - \delta z_r) \tag{3}$$

where $\varphi_e(x,y)$ and $\varphi_r(x,y)$ are the speckle phase for the excitation and reference conditions, respectively, computed using Equation 1. The δz_e and δz_r terms represent the out-of-plane differences between the two points on the object surface that image to pixel (x,y), for the excitation and reference conditions, respectively. It should be noted that the speckle phase as computed by Equation 1 ranges from 0 to 2π and may have 2π jumps, giving the resulting difference image a fringe-like appearance. If a true quantitative measurement is desired, it may be necessary to do some post-processing with a phase unwrap algorithm.

3. BAT Mask Tile Adhesive Bonding

The first application area to be evaluated involves the quality of the adhesive bonds that attach the tiles to the Swift BAT mask. The goal is to determine whether shearography methods can distinguish the poorly bonded tiles from those that are well bonded. The mask contains about 52,000 lead tiles arranged in a pseudo-random pattern, and each tile is approximately 5 mm square, 1 mm thick, and weighs about 0.25 grams. The excitation stress is a low amplitude vibration in the plane of the mask surface. The adhesive used to bond the tiles to the mask surface is somewhat flexible, and the combination of tile and adhesive can be roughly modeled as a mass on a spring that would respond to the vibration by swaying back and forth, as illustrated in Figure 2 below. The quality of the bond relates to the stiffness of the spring, which in turn determines the amplitude of motion. Based on the tile mass and a very rough estimate of the adhesive spring constant, the optimal excitation frequency was expected to be in the range of a few tens to a few hundreds of Hertz.

Good results were obtained with an excitation frequency of 180 Hz, although the exact value did not appear to be critical. The "reference" and "excitation" conditions were taken to be at 120° and -60° in the vibration cycle, representing the points where the tiles had the greatest tilt. These phase angles are with respect to the output signal of the waveform generator and compensate for any phase shift due to the shaker and the tile-"spring" combination. (Note that there are two unrelated meanings of the word phase that we are using: the speckle phase and the phase of the vibration cycle.) A set of four phase-stepped speckle images is captured both at the "reference" and at the "excitation" by strobing the laser illumination at these points in the vibration cycle. A strobe duty cycle of 25% is a good compromise between maximizing light energy to the camera and

not blurring the speckle images. The speckle phase maps for each condition are then computed, and the absolute difference between the two shows the amplitude of motion at each tile.
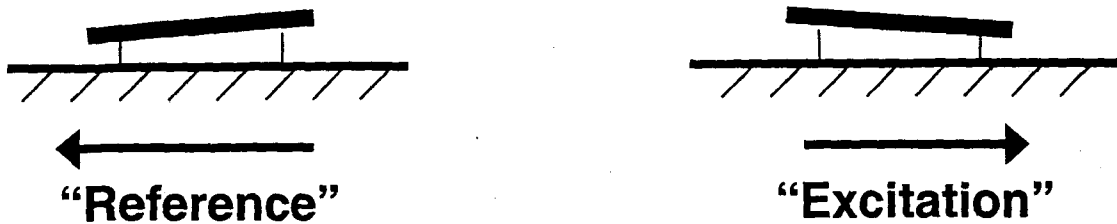

Figure 2. BAT mask tiles under vibration excitation. The "reference" and "excitation" conditions are taken to be two points in the vibration cycle, 180° apart, which give the extremes of tile tilt.

The test configuration is illustrated in Figure 3. Each image is captured with the camera operating in time-integration mode over a number of laser strobe pulses, which are synchronized with the desired vibration phase angle, reference or excitation. An integration time of 160 msec with a vibration excitation of 180 Hz provides for integration over 28 to 29 strobe pulses. Since the aperture of the camera lens must be stopped down to f/16 to get a large enough speckle size, this allows sufficient light to be accumulated for good speckle images. The strobe is generated by gating the CW laser using an acoustic-optic modulator (AOM) to direct the beam through a pin hole and onto the BAT mask. The AOM is controlled through a PC Instruments PCI-312 dual channel waveform generator board in the computer, which is also used to produce the vibration signal.

It has been assumed here that the motion of a tile under vibration is regular in the steady state so that its displacement is always the same at any particular phase angle of the vibration cycle. If this were not the case the speckles would be decorrelated over the set of strobe pulses and would tend to be smeared out. This assumption has been confirmed. (It should be noted that in cases where this assumption does not hold, the smeared speckles might provide an alternate method for identification of poorly bonded tiles.)

The vibration signal is a cosine function produced by the waveform generator board and coupled through an external power amplifier to a mechanical shaker, which drives the vibration of the BAT mask. This arrangement provides for synchronization with the acousto-optic modulator and the camera as well as allowing for the selection of all the critical parameters through the computer interface, including the frequency and amplitude of vibration and the strobe phase and dwell time.
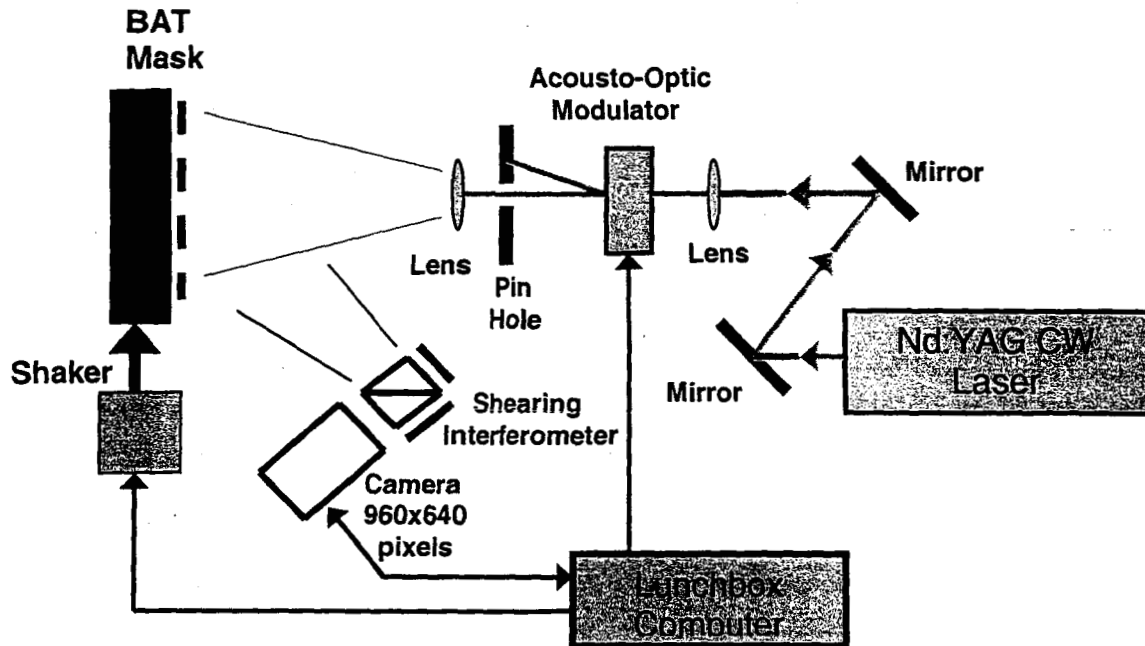
Figure 3. BAT mask test configuration. The shaker vibrates the BAT mask assembly while the acoustic-optic modulator is used to create a strobe effect with the laser beam by directing it through the pinhole and onto the mask at the appropriate point in the vibration cycle.

The experimental set up is shown in Figure 4. The BAT mask and shaker (the red and white object) are at the back toward the right side. The camera and interferometer are at the back on the left side. The acousto-optic modulator is at the right front, and the pinhole and lens are between the acousto-optic modulator and the BAT mask. The laser is not shown. A close up of the BAT mask, illuminated by the laser, with the shaker to its right is shown in Figure 5. To provide a reasonable light level for the camera the laser illumination area was chosen to be about 15 cm in diameter. It should be noted that gating with a CW laser is a rather inefficient since the duty cycle only 25%. The acoustic-optic modulator also introduces inefficiencies in that only one of the diffraction lobes can be utilized. A possible alternative would be to use a pulsed laser whose pulse could be externally controlled by the computer.
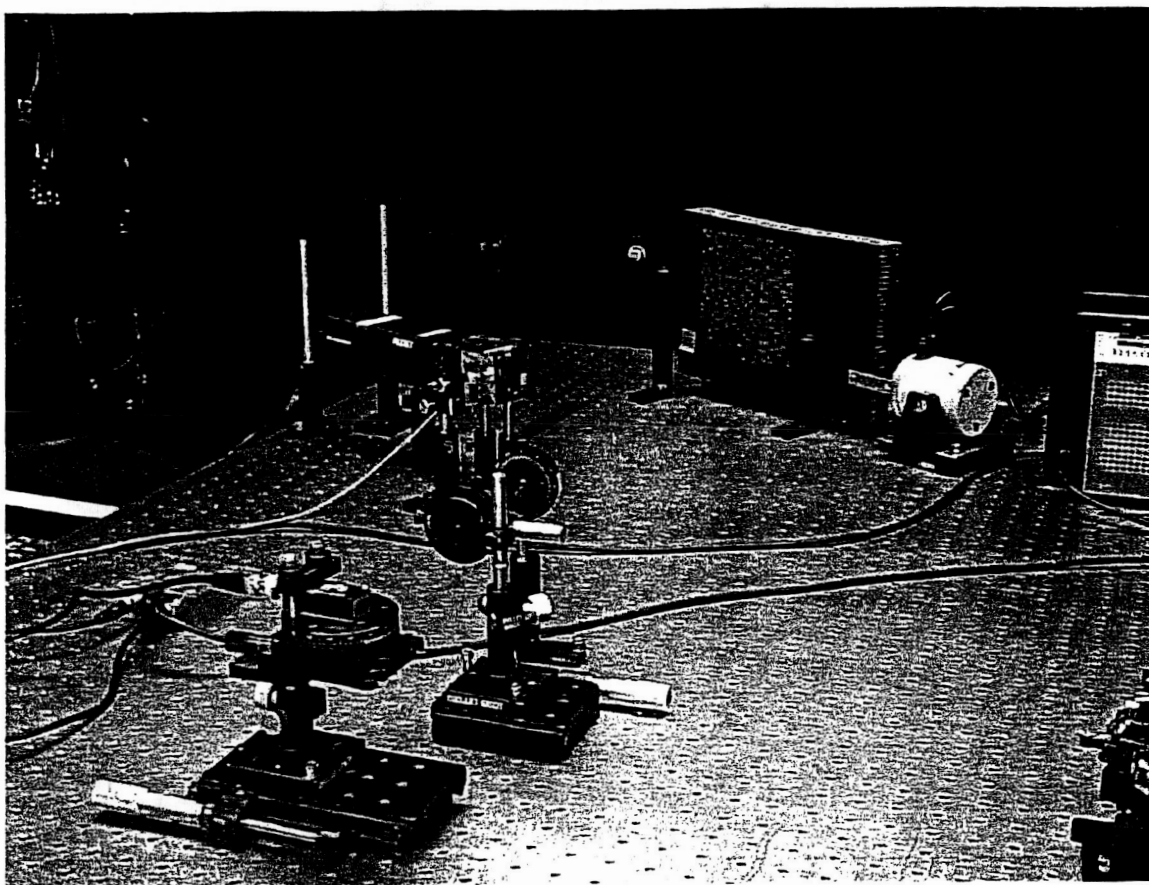
Figure 4. BAT mask experimental set up. The BAT mask is in the back with the shaker (the red and white object) to the right of it. The camera and interferometer are in the back at the left, and the acousto-optic modulator is at the left front. The pinhole and lens are between the acousto-optic modulator and the BAT mask. The laser is not shown here.
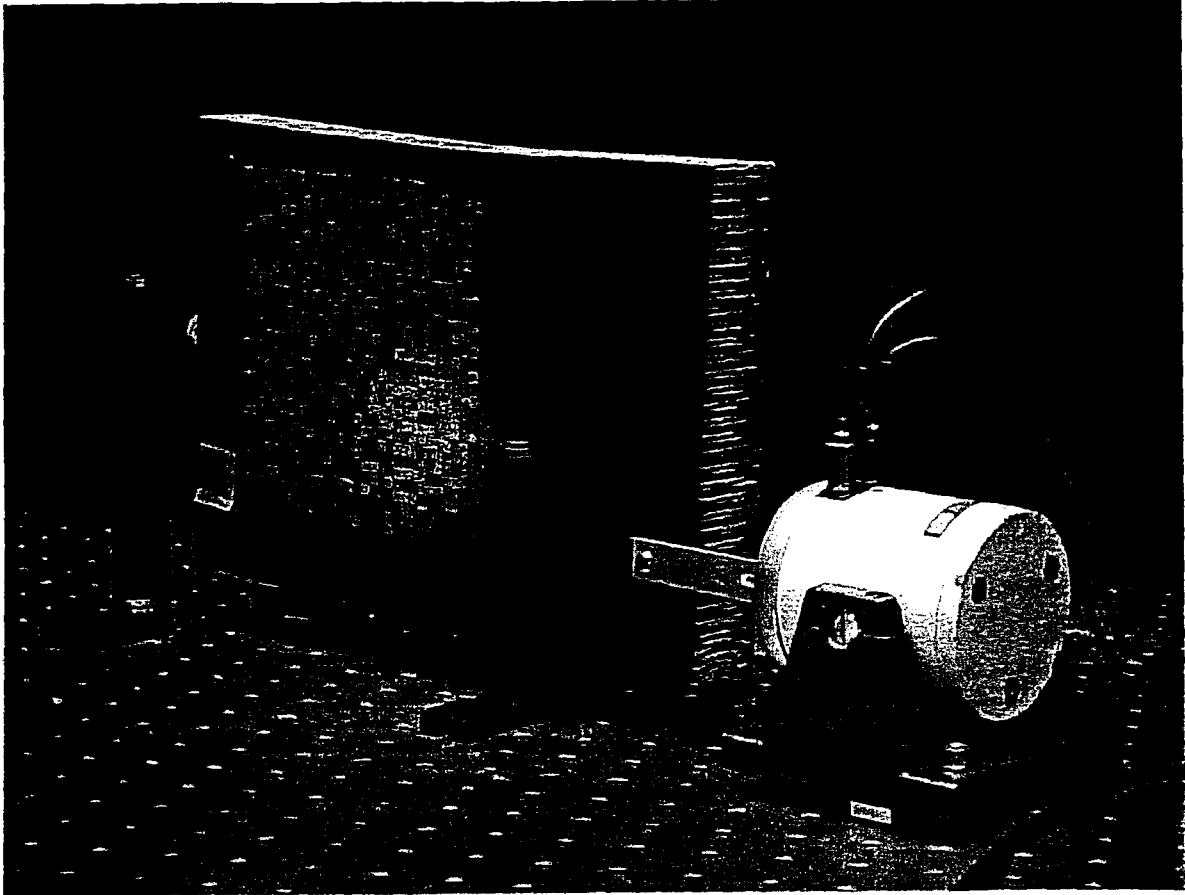
Figure 5. Portion of the BAT mask under test, illuminated by laser light and attached to a mechanical shaker. The tiles appear as a pseudo-random pattern of small gray squares. The orange spots are patches of adhesive where the tiles have fallen off.

Figure 6 shows a sheared white light image of the BAT mask as seen through the interferometer by the camera. The horizontal shear displacement, which is about 1 mm (20% of the tile size), makes the image looks blurred. Figure 7 is a sheared image captured in laser light, illustrating the speckle inherent in such an image. Also apparent in this image is the limit of laser illumination, the roughly circular area in the right two-thirds of the picture, where good results can be obtained. This particular image corresponds to the first phase step for the reference condition (at 120° in the vibration cycle). Three other speckle phase step images, which are not shown, are also taken for the reference condition. These would look the same as the first image but are actually quite different in the speckle pattern detail. These four images are then used to compute a speckle phase map for the reference condition, which is shown in Figure 8. Notice that in the phase map, individual tiles are not seen, indicating that effects due to variations in illumination and reflectivity across the surface are removed when the speckle phase is computed.
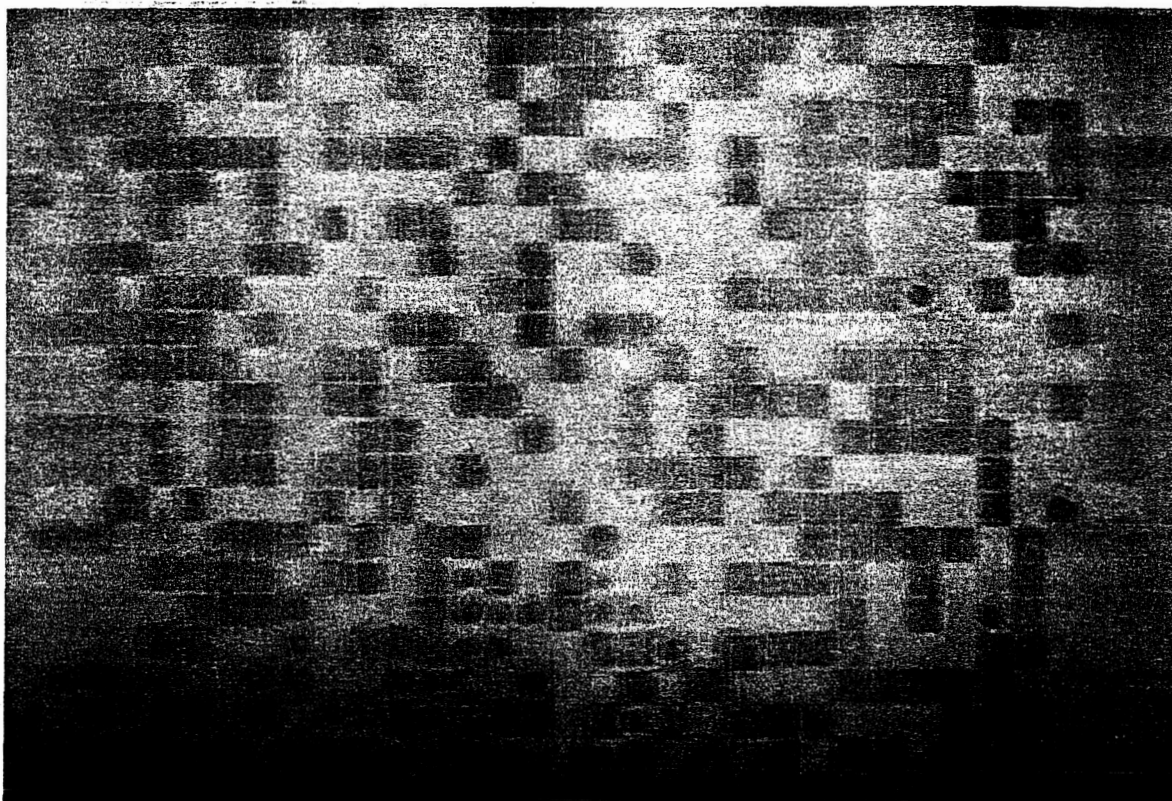
Figure 6. White light image of the BAT mask as seen through the interferometer by the camera. The image is sheared horizontally by about 1 mm making it appear blurred.

The phase map for the excitation condition (at -60 degrees in the vibration cycle) would appear very similar to the one in Figure 8 for the reference; however, they are again quite different in the speckle details. The differential displacement, which is shown in Figure 9, is obtained by taking the absolute difference, pixel by pixel, of the reference and excitation speckle maps. The tiles with the greatest range of motion are readily apparent against the almost uniform dark background in this figure. Note that the region with the dark background is the area where there is sufficient illumination. Dark areas, with differential displacement close to zero, represent those parts of the mask where there is no change in the phase map, which implies no (or very little) change in the surface slope. These may be areas with no tiles or with tiles that are very well bonded. In the outer portion of the figure (the area with the speckle background), the illumination is not strong enough to produce a good phase map, and the speckle there is useless noise.

The figures described here were obtained at a vibration frequency of 180 Hz. It was anticipated that tiles with different quality bonding might respond differently to different excitation frequencies. We note, however, that results appeared fairly uniform over a range of frequencies, and no strongly resonant features were apparent. This might be because the emphasis during testing was on visual identification of loose tiles (see the discussion below on the pull test) or because the test did not cover a broad enough range of frequencies.
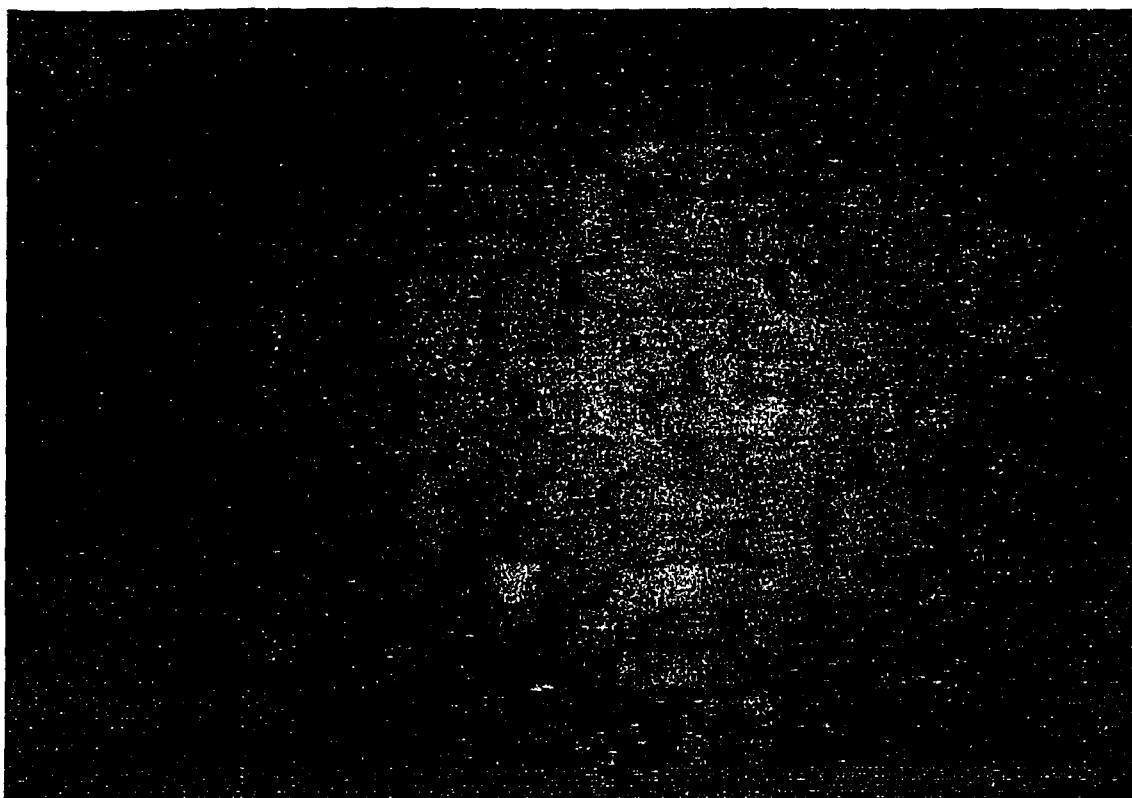
Figure 7. Typical sheared image of the mask acquired under laser light. This particular image is for the reference condition (at 120 degrees in the vibration cycle) and is the first in the series of four phase-stepped images for that condition. All the images of this type appear to be identical but are actually quite different in the speckle pattern details.

Generally speaking, the vibration amplitude seemed to be more critical than the frequency. For good identification the amplitude must be set low enough that no motion appears in either the well bonded tiles or the background structure to which the tiles are attached. This allows the poorly bonded tiles to clearly stand out in the differential displacement image. As a practical matter the amplitude is not well regulated by the voltage output from the waveform generator because of variation in the frequency response of the shaker. However, a reasonable adjustment can be obtained by turning up the amplitude until motion is seen throughout the whole imaged area, including the background structure, and then backing off.

In many inspection applications, shearography is used to visually identify whether or not the object has failed, and all of the poorly bonded tiles stand out pretty clearly in Figure 9. In order to put the results on a more quantitative basis, a pull test was performed on a number of tiles for comparison with the shearography results. To assure a straight pull, a flat head nail was attached to the tiles with super glue as a pull mechanism. As each tile was pulled to failure, the force was measured with a load cell and automatically stored on computer for analysis. The test set up is shown in Figure 10.
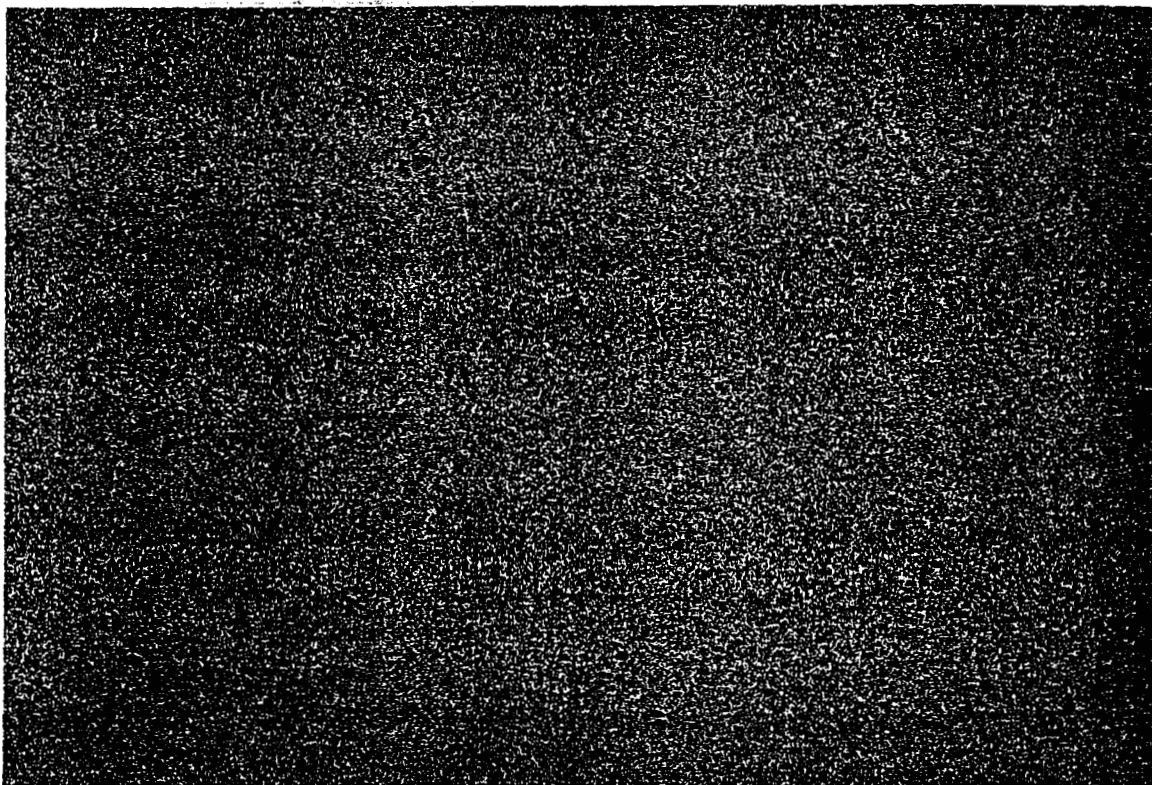
Figure 8. Typical speckle phase map computed from the four phase-stepped images. This is for the reference condition (120 degrees in the vibration cycle), but the phase map for the excitation condition has the same general appearance.
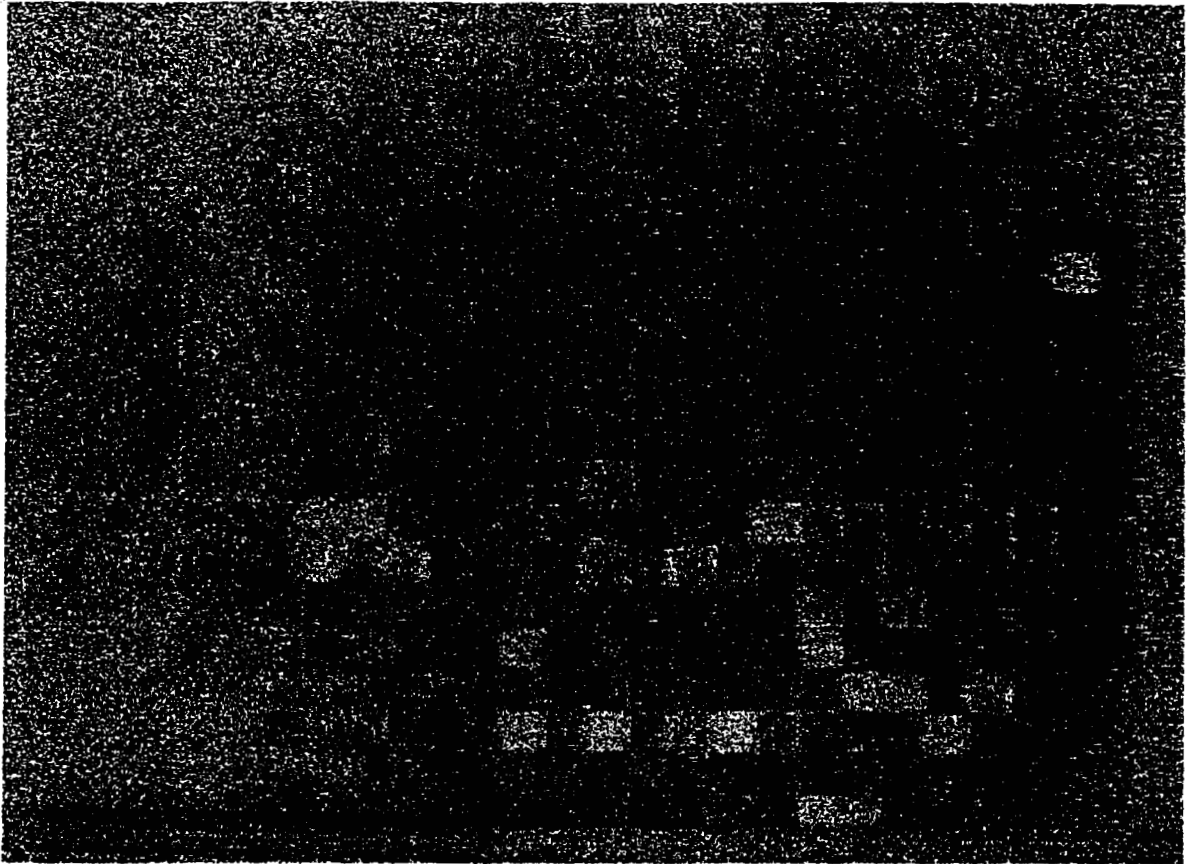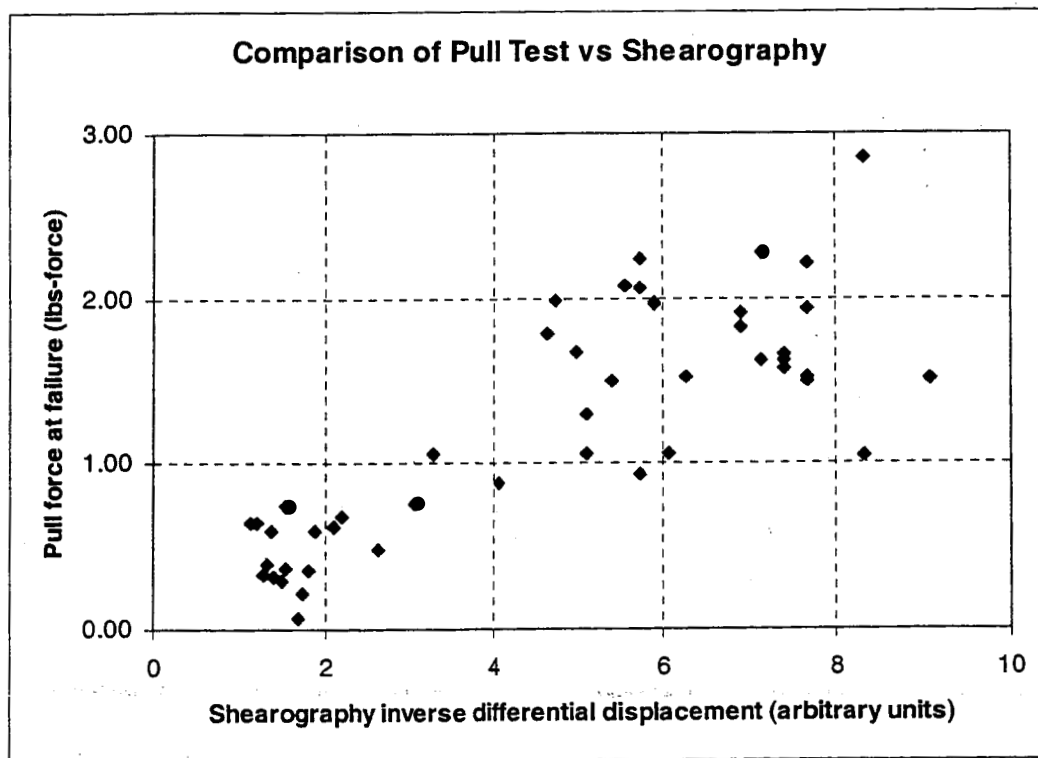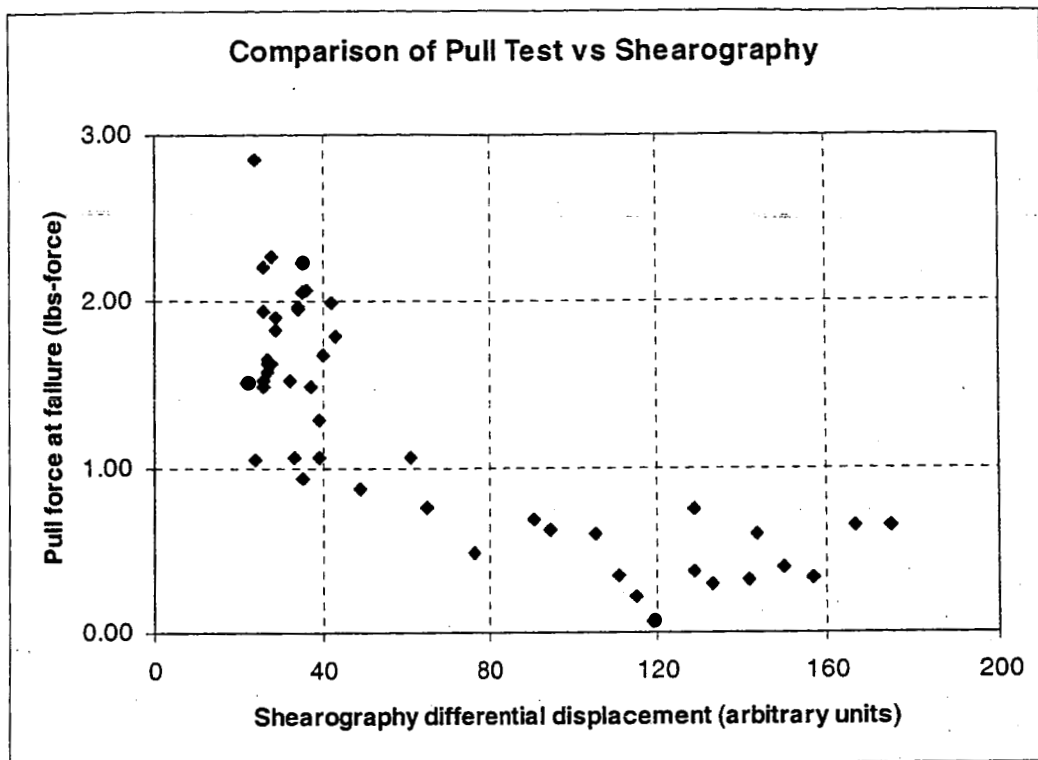
Figure 9. Differential displacement, computed by taking the difference between the reference and excitation speckle phase maps (120 and -60 degrees in the vibration cycle, respectively). The tiles that have the greatest range of motion stand out against the relatively uniform dark background. The vibration frequency is 180 Hz.
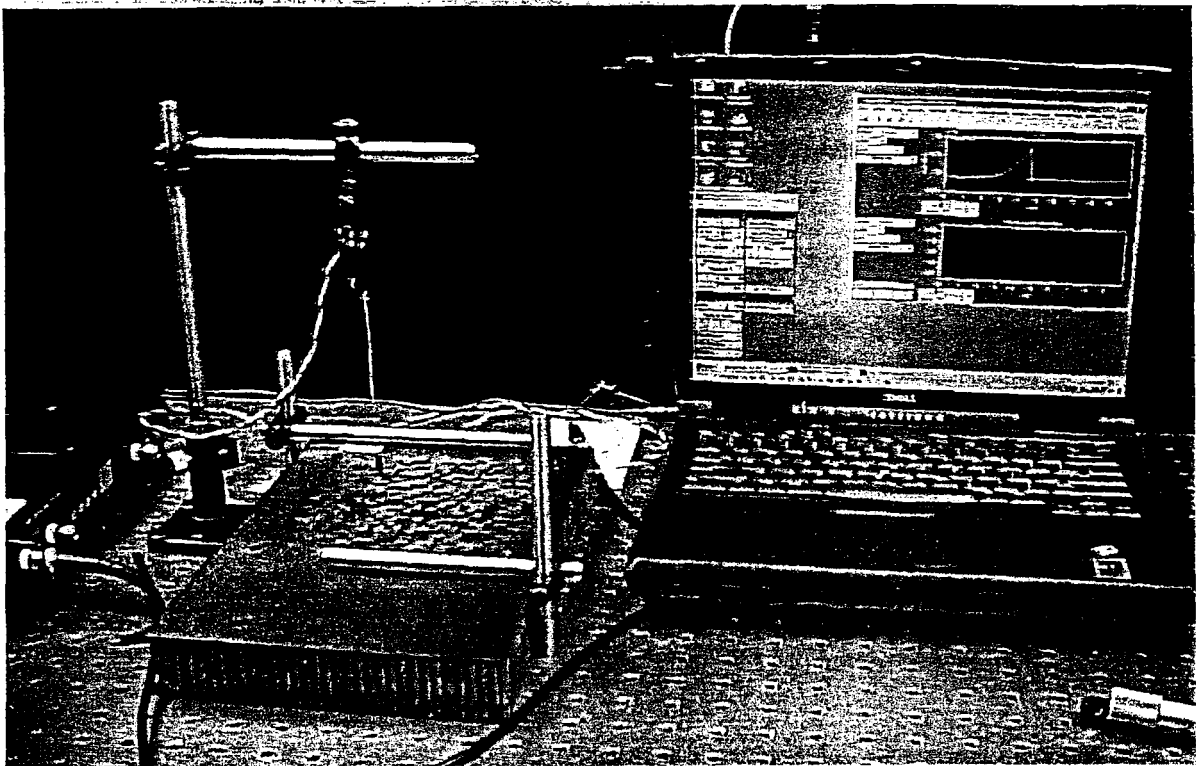
Figure 10. BAT Mask tile pull test set up.

A scatter graph of pull force versus the shearography differential displacement, where each point represents a tile, is shown in Figure 11. The differential displacement was computed from the gray scale image of Figure 9 by averaging over an 11 x 11 block of pixels at the center of each tile. A nearly inverse relationship is apparent in the graph. The graph of inverse differential displacement (bottom of Figure 11) then becomes roughly linear, although the points spread out at the upper end because the displacement becomes small there and random error is accentuated in the inverse. A regression analysis gives a linear fit of the form $y = m x + b$ with $m = 0.223$ and $b = 0.185$, where x is the inverse differential displacement and y is the pull test result in pounds. The standard errors of m and b are 0.0226 and 0.122, respectively, and the coefficient of determination, R^2, is 0.673. It is anticipated that increasing the vibration amplitude would generally increase the base level differential displacement of all the tiles, resulting in a tighter linear fit.

Figure 11. Pull test results compared to the shearography differential displacement results of Figure 9, averaged over the center of each tile. The bottom plot uses inverse differential displacement, which results in a roughly linear relationship with pull force.
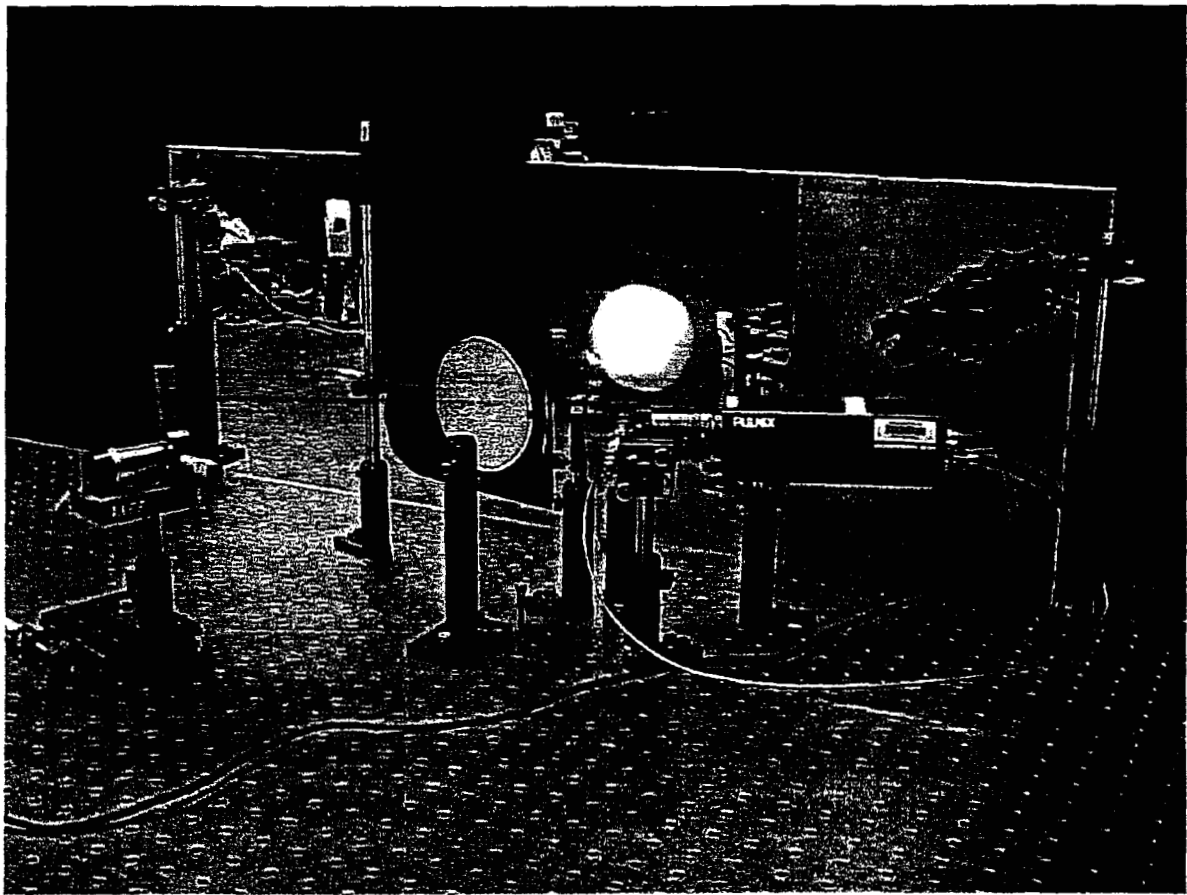
4. Specular Surface Honeycomb Panel

As noted earlier, shearography has been demonstrated to give good results with diffuse surface honeycomb panels in identifying bonding failures between the core and skin. Vacuum, pressure, and thermal excitation have been used successfully. At the cell walls of the honeycomb core, where the skin is attached, the surface is constrained, and no change in slope can occur in response to the excitation. At the interior of the cells, however, the surface is free to respond and will appear different in the display of differential surface gradient. With a well bonded structure, the distinct honeycomb pattern of the core stands out in the display, and any bonding failure is readily apparent as an interruption of that pattern. In the present application, however, the primary challenge appeared to be that the panels have a specular surface and do not produce the speckle patterns needed for shearography. The approach we used was to generate the speckles by illuminating some other diffuse surface with laser light and then use the specular surface as a mirror to view them. In principle, this configuration should produce a display very similar to that obtained from a diffuse surface honeycomb panel.

The most appropriate excitation appears to be a slight pressure applied from inside the honeycomb core. The core has a system of holes that allow the pressure to equalize over the interior cells; however, all external holes must be sealed. A vacuum excitation from outside the panel was considered but appeared to be impractical because the specular surface was not supposed to be touched and a special vacuum chamber would need to be constructed to fit the panel and seal at the edges. In addition, the sample panel was in rather poor condition and would have been difficult to seal up this way.
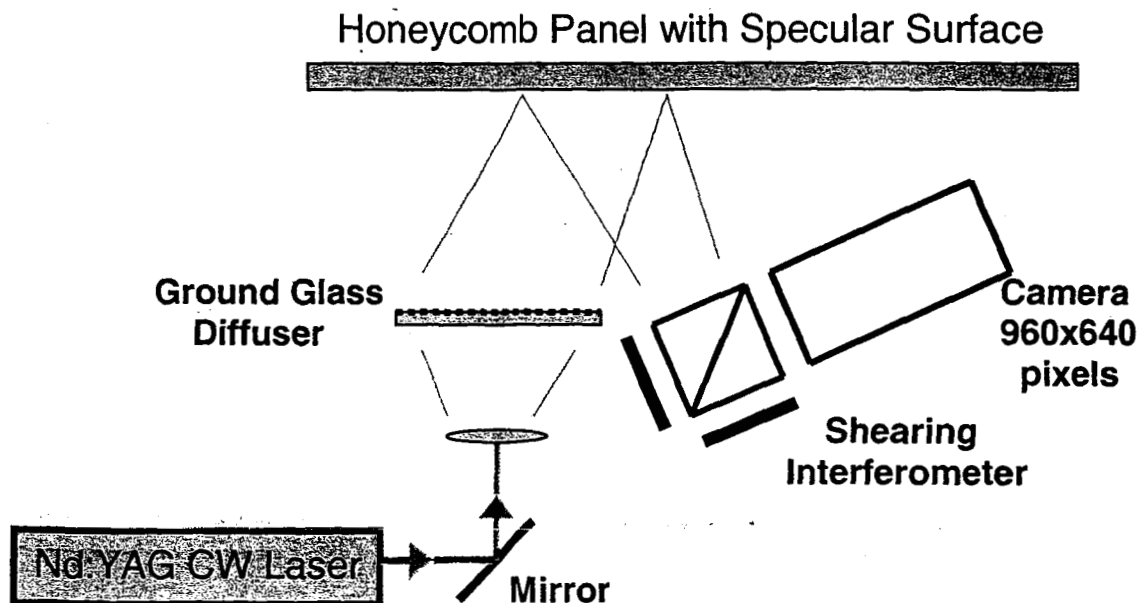
Figure 12. Specular surface honeycomb panel test configuration. The speckle is generated by passing the laser light through the ground glass diffuser and imaged using the specular surface as a mirror.

The experimental configuration is illustrated in Figure 12. The speckles are generated by expanding the laser beam and passing it through a ground glass diffuser. The diffuser is then imaged through the specular surface, using it as a mirror. Figure 13 shows the actual test set up. The laser light comes in from the left and passes through the microscope objective and pinhole at the left side of picture to the ground glass diffuser, which is seen as the green circle to the left of center. The honeycomb panel is mounted vertically at the back edge of the optical table. The skin of the panel consisted of two layers, a fiberglass underlayer that was bonded directly to the core, with a top layer of aluminum, which was bonded to the fiberglass and polished to a mirror surface. As seen in Figure 13, portions of the specular aluminum layer had been stripped away. The image of the diffuser, reflected by the specular surface, is the bright green spot (right of center), and the interferometer and camera appear in front of the diffuser image.

Figure 13. Specular surface honeycomb panel test set up. The laser light comes in from the left and passes through the microscope objective and pinhole (left side of picture) to the ground glass diffuser (green circle left of center). The honeycomb panel is mounted vertically at the back edge of the optical table, and the image of the diffuser, reflected by the specular surface, is the bright green spot (right of center), and the interferometer and camera appear in front of the diffuser image. Portions of the specular aluminum coating had been stripped away, revealing the fiberglass underlayer.

Ideally for non-destructive evaluation of these structures, it is desirable to have a positive verification that the structure is sound by identifying the characteristic honeycomb pattern in the differential displacement display. We were unable to obtain such a pattern; however, we were able to identify areas where large-scale bonding failures were readily apparent. In Figure 14, for example, the speckle fringe pattern indicates an area, roughly 4 to 6 cm across, that was not bonded. This was verified by destructively cutting through the skin, where we found that the bonding between the fiberglass and the core had failed, although the aluminum to fiberglass bond appeared intact.

The difficulty in imaging the honeycomb pattern is apparently due to the very small cell size of the core (about 3 mm), with the double layer composition of the skin possibly a contributing factor. In order to see the surface deflection fringes at this cell size, the shear distance must be less than 1 mm, greatly reducing the sensitivity of the system. In addition, a fringe pattern of that scale tends to disappear in the speckle noise. It should be noted that these effects are not related to the method of imaging through the specular surface. This was demonstrated by the fact that very similar results were obtained when a standard shearography configuration was used to examine a portion of the panel where the specular layer had been stripped away, leaving the underlying diffuse fiberglass layer exposed. Our results indicate that the general principle of using the surface as a mirror to image the speckles is valid approach, extending the applicability of shearography to a new class of objects that could not be handled with the traditional technique.

It might be possible to get fringe resolution at the scale of the cell size by reconfiguring the imaging optics to magnify the apparent cell size in the image. This is most readily done with a longer focal length lens on the camera. It would probably be desirable to also increase the pixel count of the camera so that a larger area of the surface can be examined at a time, although this would not be necessary to demonstrate the suitability of shearography to this particular application. It should be pointed out that the double layer skin, particularly the stiffness of the aluminum layer combined with the small cell size, might also affect the ability to display a good pattern.

For the specular surface honeycomb panel, the technique of generating speckles with some other diffuse surface and imaging them through the mirror-like panel surface appears to be valid. This technique opens up the use of shearography to a new class of objects that could not have been examined using more traditional shearography configurations. The results obtained here are encouraging, but further development should be undertaken to demonstrate the general applicability of the technique and to establish a firm quantitative foundation.

Regarding the application of shearography to the non-destructive evaluation of the particular honeycomb panel, it has been demonstrated that large scale bonding failures can be identified with the system as configured. However, to reduce the scale size that can be evaluated to match the honeycomb core cell size, the optical configuration should be modified to increase the image size of the surface under test.

6. References

[1]   G. Lu, B.A. Bard, and S. Wu, "A Real-time Portable Phase-stepping Shearography System for NDE," *Proc. Soc. Photo-Opt. Instrum. Eng.*, **3397-25**, 1998.

[2]   B. A. Bard, "Laser-Modulated Phase-Stepping Digital Shearography for the Quantitative Analysis of Structural Vibration," Ph.D. Thesis, The Pennsylvania State University, August 1997.

[3]   J. W. Goodman, "Statistical Properties of Laser Speckle Patterns," in J. C. Dainty, Ed., *Laser Speckle and Related Phenomena*, Springer-Verlag, 1984.

Figure 14. Specular honeycomb panel with bonding failure. The fringes indicate large scale areas where the skin is not bonded to the core. The lighter gray area below the fringe pattern is thought to be a region of good bonding.

5. Conclusions and Recommendations

In the evaluation of tile bonds on the BAT mask, the system was able to pretty clearly identify the tiles that were poorly bonded and appears to be effective for non-destructive evaluation in that application. For the full size mask, however, a fixture would need to be constructed to hold the mask while the vibration is applied. Since the mask is quite large, it is unlikely that inspection could be conveniently done in a single pass. It would be necessary to examine the mask in a sequence of spots, which would probably be most easily done by moving the mask rather than the inspection system. Because of the inherent robustness of shearography measurements, this should not be difficult. There is no need for the system to be set up on an optical bench; only the camera and interferometer would need to be mounted together on a small rigid plate.

The "spot size" (the area that can be examined at one time) could be scaled up by using a more powerful laser, particularly a pulsed laser as described below, and/or by allowing the camera to integrate over a longer time period. A system intended specifically for large area vibration analysis should incorporate a pulsed laser and eliminate the acousto-optic modulator, which would greatly increase the optical efficiency, with a corresponding increase in the spot size.